THE JOURNAL OF BIOLOGICAL CHEMISTRY VOL. 280, NO. 47, pp. 39324–39331, November 25, 2005
© 2005 by The American Society for Biochemistry and Molecular Biology, Inc. Printed in the U.S.A.

Self-association of Transmembrane α-Helices in Model Membranes

IMPORTANCE OF HELIX ORIENTATION AND ROLE OF HYDROPHOBIC MISMATCH[*][S]

Received for publication, March 15, 2005, and in revised form, September 13, 2005 Published, JBC Papers in Press, September 15, 2005, DOI 10.1074/jbc.M502810200

Emma Sparr[‡1], **Walter L. Ash**[§2], **Petr V. Nazarov**[¶], **Dirk T. S. Rijkers**[‖], **Marcus A. Hemminga**[¶], **D. Peter Tieleman**[§3], **and J. Antoinette Killian**[‡]

From the [‡]*Department of Biochemistry of Membranes, Institute of Biomembranes and Bijvoet Center for Biomolecular Research, and* [‖]*Department of Medicinal Chemistry, Faculty of Pharmaceutical Sciences, Utrecht University, Padualaan 8, NL-3584 CH Utrecht, The Netherlands, the* [§]*Department of Biological Sciences, University of Calgary, Calgary, Alberta T2N 1N4, Canada, and the* [¶]*Laboratory of Biophysics Wageningen University, P. O. Box 8128, 6700 ET Wageningen, The Netherlands*

Interactions between transmembrane helices play a key role in almost all cellular processes involving membrane proteins. We have investigated helix-helix interactions in lipid bilayers with synthetic tryptophan-flanked peptides that mimic the membrane spanning parts of membrane proteins. The peptides were functionalized with pyrene to allow the self-association of the helices to be monitored by pyrene fluorescence and Trp-pyrene fluorescence resonance energy transfer (FRET). Specific labeling of peptides at either their N or C terminus has shown that helix-helix association occurs almost exclusively between antiparallel helices. Furthermore, computer modeling suggested that antiparallel association arises primarily from the electrostatic interactions between α-helix backbone atoms. We propose that such interactions may provide a force for the preferentially antiparallel association of helices in polytopic membrane proteins. Helix-helix association was also found to depend on the lipid environment. In bilayers of dioleoylphosphatidylcholine, in which the hydrophobic length of the peptides approximately matched the bilayer thickness, association between the helices was found to require peptide/lipid ratios exceeding 1/25. Self-association of the helices was promoted by either increasing or decreasing the bilayer thickness, and by adding cholesterol. These results indicate that helix-helix association in membrane proteins can be promoted by unfavorable protein-lipid interactions.

Most membrane proteins have one or more hydrophobic segments that span the membrane in an α-helical conformation. Interactions between these transmembrane (TM)[4] helices are important for determining the structure of multispanning membrane proteins and for assembly of membrane proteins into oligomeric structures (1–4). Several factors are thought to be responsible for the association of helices in membrane proteins, including surface complementarity, the presence of polar residues in the transmembrane region (5–7), and certain specific motifs such as the well known *GXXXG* pattern (8, 9). It is likely that several of these factors act in concert to determine the final folded structure, or the association of monomers to form an oligomer.

In addition to helix-helix interactions, interactions between the helices and surrounding lipids also play a role in the organization and assembly of TM helices. For example, even when helices do not exhibit any tendency to undergo specific association (10–12), helix-helix association could still occur as a result of poor packing between the lipids and helices, or from a favorable change in entropy resulting from the release of helix-bound lipids upon helix association. In these cases, helix association is primarily driven by lipid-protein interactions rather than strongly favorable protein-protein interactions. It is likely that in real membrane proteins the driving forces for folding involve both types of interaction, whether or not specific protein-protein recognition motifs are present.

One property of a protein-lipid system that is known to affect helix-helix association is the extent of matching between the hydrophobic length of the helices and the hydrophobic thickness of the lipid bilayer. In the case of hydrophobic mismatch, helix-helix interactions may be promoted because of relatively unfavorable lipid-helix interactions. It was previously shown with Lys-flanked TM peptides that hydrophobic mismatch does promote self-association, both when a helix-helix recognition motif is present (13), and in the absence of such a motif (14, 15). However, it is still not clear whether or not helix-helix association can be considered a general response of TM helices to mismatch. This is because many other responses to hydrophobic mismatch can also occur (reviewed in Refs. 16 and 17), such as ordering/disordering of the lipid acyl chains, alterations in helix tilt angle, adaptations of the peptide backbone, and because it has been shown that the type and extent of the responses that occur depend on the composition of the TM helix. For example, Trp-flanked peptides, which were designed to mimic the membrane spanning parts of intrinsic membrane proteins, showed very different responses to hydrophobic mismatch than analogous Lys-flanked peptides (14, 15).

The aims of the present study are to establish whether or not increased association is a general property of transmembrane segments under conditions of hydrophobic mismatch, and to understand the molecular details of any oligomers that are formed. We investigated the association between Trp-flanked peptides that were designed to mimic

* This work was supported in part by the Canadian Institutes of Health Research. The costs of publication of this article were defrayed in part by the payment of page charges. This article must therefore be hereby marked "*advertisement*" in accordance with 18 U.S.C. Section 1734 solely to indicate this fact.

[S] The on-line version of this article (available at http://www.jbc.org) contains supplemental Table A.

[1] Supported by The Swedish Foundation for International Cooperation in Research and Higher Education. To whom correspondence may be addressed. Present address: Physical Chemistry 1, Center for Chemistry and Chemical Engineering, Lund University, P.O. Box 124, SE-221 00 Lund, Sweden. Tel.: 46-0-46-222-48-12; Fax: 46-0-46-222-44-13; E-mail: emma.sparr@fkem1.lu.se.

[2] Supported by an Alberta Heritage Foundation for Medical Research studentship and a National Sciences and Engineering Research Council Canada Graduate Scholarship. To whom correspondence may be addressed. Present address: Biological Sciences 405, 2500 University Drive NW, Calgary T2N 1N4, Canada. Tel.: 403-220-4039; Fax: 403-289-9311; E-mail: wlash@ucalgary.ca.

[3] Alberta Heritage Foundation for Medical Research Senior scholar, Canadian Institutes of Health Research New Investigator.

[4] The abbreviations used are: TM, transmembrane; FRET, fluorescence resonance energy transfer; r.m.s., root mean square; PC, phosphatidylcholine; HPLC, high performance liquid chromatography; E/M, excimer/monomer ratio.

the transmembrane segments of real membrane proteins, without specific helix-helix recognition motifs. These model peptides allowed us to focus on nonspecific forces involved in membrane protein structure and stability. The peptides were functionalized with pyrene to allow monitoring of association by pyrene fluorescence and Trp-pyrene FRET. By labeling peptides at either their N or C terminus, we show that helix-helix association occurs almost exclusively between antiparallel helices. We also show that hydrophobic mismatch promotes helix-helix association. Our theoretical models show that the antiparallel association of helices is promoted by favorable electrostatic interactions between α-helix backbone dipole moments. These results contribute to our understanding of the role of protein-protein and protein-lipid interactions in determining the association of transmembrane segments in membrane proteins. The implications of these findings for assembly and stability of membrane proteins and membrane protein complexes are also discussed.

EXPERIMENTAL PROCEDURES

Materials—1,2-Dioleoyl-*sn*-glycero-3-phosphocholine (C18:1_c-PC), 1,2-dimyristoleoyl-*sn*-glycero-3-phosphocholine (C14:1_c-PC), 1,2-dierucoyl-*sn*-glycero-3-phosphocholine (C22:1_c-PC), and cholesterol were obtained from Avanti Polar Lipids (Alabaster, AL). The pyrene-labeled peptides pyr_N-WALP23 (Ac-C(pyrene)-GWW$(LA)_8$LWWA-amide) and pyr_C-WALP23 (Ac-GWW$(LA)_8$LWWGC(pyrene)-amide) were synthesized as described earlier (18). The fluorescent probe *N*-(1-pyrene)maleimide was obtained from Molecular Probes Europe BV (Leiden, The Netherlands). The peptides were purified by high performance liquid chromatography (HPLC). Their identity was confirmed by mass spectrometry and their purity was established by analytical HPLC to be better than 95%. Milli-Q water was used for all experiments.

Sample Preparation—Fluorescence experiments were performed on multilamellar vesicles with peptide/lipid ratios between 1/10 and 1/3000. The lipids were dissolved in either chloroform/methanol (1/1) or chloroform, and the peptides were dissolved in 2,2,2-trifluoroethanol. The concentration of WALP in the stock solution was determined from the absorbance at 280 nm using an extinction coefficient of 21,300 M^{-1} cm^{-1}. Phospholipids were quantified according to Rouser *et al.* (19).

Peptides were incorporated into lipid vesicles essentially as described (20). Stock solutions of peptide and lipids were mixed in the desired peptide/lipid ratio. The solvent was removed by evaporation under a stream of nitrogen and the peptide/lipid film was further dried overnight under vacuum. The mixed films were hydrated in Milli-Q water to a final peptide concentration of 0.25 μM, and the samples were dispersed by vigorous vortexing. The samples were then subjected to 10 cycles of freeze-thawing. The resulting multilamellar vesicles were stored at 4 °C until use. Circular dichroism measurements confirmed that the labeled WALP peptides were incorporated to form stable TM helices in lipid bilayers.

Fluorescence Experiments—Fluorescence experiments were performed with an SLM Aminco SPF-500 C fluorimeter. All samples (1.2 ml) were continuously stirred in a 10 × 4-mm quartz cuvette. The temperature was maintained at 22 °C via a water bath with continuous circulation. In addition, the absorbance of each sample was measured at the wavelengths of excitation and emission on a PerkinElmer UV-visual Lambda 18 spectrometer. These data were used to calculate the inner filter effect (21).

The fluorescence emission of pyrene was studied with spectral recordings between 370 and 600 nm (bandwidth 5 nm) with an excitation wavelength of 350 nm (bandwidth 5 nm). The FRET efficiency between Trp and pyrene was determined from the degree of Trp (donor) quenching. Fluorescence spectra were recorded between 320 and 550 nm (bandwidth 5 nm) with an excitation wavelength of 280 nm (bandwidth 5 nm). In this assay, both Trp (donor) and pyrene (acceptor) were present in the same peptide, implying that the detected Trp quenching includes contributions both from intermolecular energy transfer and from intramolecular energy transfer. The contribution from the intramolecular Trp quenching was estimated from FRET data obtained for C18:1_c-PC vesicles with very low peptide concentrations (0.03–0.2%). In these systems, the Trp quenching was virtually constant, and the intramolecular FRET could therefore be considered constant. The FRET data presented in this study are given as the ratio of the Trp intensity to the intensity where there is only intramolecular energy transfer.

Theoretical Fluorescence Resonance Energy Transfer—Fluorescent data were analyzed by means of simulation-based fitting, which produces an approximation of experimental data by a simulated analogue (22, 23). In the modeling the peptides are assumed to be perfectly α-helical (23), and the location of the four Trp donors and pyrene acceptors is derived from the primary sequences. The distances from the C_α at the helix backbone to the centers of moiety of the donors and acceptors were estimated to be 3.0 and 6.0 Å, respectively. As a model for peptides incorporated into a lipid bilayer, a square region of a bilayer containing 200 peptides was considered. The peptides were located on the points of a triangular lattice (assuming hexagonal packing) with the closest distance between points set to 10 Å. Lipids were not explicitly included in the model, however, their average diameter (7.5 Å) and the peptide/lipid ratio were used to define the final size of the peptide-lipid model. Peptides were randomly directed with the helix axis of the peptide either parallel or antiparallel to the normal of the membrane.

For each *i*-th donor in this model, the probability of energy transfer to one of the acceptors is given by the following equation,

$$p_i^{ET} = \frac{\sum_j (R_0/R_{i,j})^6}{1 + \sum_j (R_0/R_{i,j})^6} \qquad \text{(Eq. 1)}$$

where $R_{i,j}$ is the distance between the *i*-th donor and *j*-th acceptor in the system, and R_0 is the Förster distance, which was set to 28 Å (21). The summation runs over all the acceptors in the system. The mean value $<p^{ET}>$ for all donors gives the total energy transfer efficiency in the peptide-lipid model. The protein insertion and FRET simulation were repeated 50 times and averaged to give the final result.

Computer Modeling and Structure Prediction—Dimers of WALP23 (Ac-GWW$(LA)_8$LWWA-amide) were modeled with a simulated annealing modeling protocol (24), using the force field and methodology previously described (25). We performed four different modeling runs in which the peptides were either oriented parallel or antiparallel to each other, and in which the helix dipole moments were either treated normally or artificially reversed. The latter was done by reversing the sign of the partial charges on all C=O and N–H backbone atoms on one helix. This backbone treatment did not detectably alter the structure of individual helices (not shown). The modeling runs were labeled AA, PP, AP, and PA, where the first letter denoted the physical orientation and the second the dipole orientation. Thus AP and PA had helix dipole moments that were uncoupled from packing. Each starting structure was a pair of ideal α-helices, 1.04 nm apart. Thirteen starting orientations, generated from evenly distributed symmetric rotations of the helices around their main axes, were used to generate 125 structures each, resulting in a total of 1625 structures for each model. Extremely high-energy structures resulting from instabilities during annealing were dis-

carded, amounting to less than 20 structures for each case. In all cases, the last turn of the helix had its four unsatisfied hydrogen bond donors or acceptors "turned off" by setting the partial charge of both atoms in the N–H or C=O moieties to zero. This was done to restrict unrealistically strong electrostatic interactions between the unshielded termini, which would ordinarily be solvated by water or involved in interactions with the lipid head groups.

Crossing angles and helix-helix separation distances were calculated using the TWISTER algorithm (26), averaged over 8 center-most residues. We calculated the propensity for each amino acid to reside in the helix-helix interface by summing intermolecular contacts by residue type. The interhelical contact values indicate the total number of residues of a particular type, in the entire 1625 structure ensemble, that formed one or more intermolecular contacts with an atom-atom distance less than 0.4 nm, a value determined empirically with visual inspection of the resulting interface definitions. Multiple contacts made by a single residue (uniquely defined in terms of dimer model number, monomer, and sequence position) were only counted once.

Clustering followed a two-tiered protocol. Initial clusters were assigned based on crossing angle, helix-helix separation distance, and the fraction of buried Ala calculated as described above. These primary clusters were refined with a second round of clustering based on atomic coordinates. For the initial coarse-level clustering, Hierarchical Clustering Explorer 3.0 (27) was used with average linkage clustering and the Euclidian distance similarity scoring function on normalized data. The minimum similarity cut-off was set to 0.901, chosen to yield at least 20–30 clusters for each data set. All clusters containing more than 100 members were selected and subclustered based on the root mean square deviation (r.m.s. deviation) of the atomic coordinates of all non-hydrogen atoms between least-squares fit structures, using the program NMRCLUST (28) and an r.m.s. deviation cut-off of 0.3 nm. A subset of the data, corresponding to the first 40 structures generated for each initial starting orientation of the helices (or 520 structures for each model), was also clustered using the r.m.s. deviation-based method with NMRCLUST. This subset analysis was conducted as a check against the two-tier process described above.

RESULTS

Helix-Helix Association as Analyzed by Pyrene Excimer Fluorescence—We investigated the interactions between Trp-flanked TM α-helices by using pyrene-labeled WALP peptides. The pyrene monomer exhibits a characteristic fluorescence emission spectrum with three maxima at wavelengths between 375 and 420 nm. When two pyrene rings are in close contact with each other, they form an excited state dimer (excimer), which exhibits a unique fluorescence peak at a wavelength of about 490 nm.

The helix-helix interaction was first studied in multilamellar vesicles consisting of C18:1_c-PC and the N-terminal labeled peptide pyr_N-WALP23 at peptide/lipid ratios ranging from 1/3000 to 1/10. Surprisingly, the recorded pyrene emission spectra showed no dependence on the peptide/lipid ratio. Only the monomer emission peak was observed, and excimer formation could not even be detected at high peptide concentrations (Fig. 1). This suggests that there is no interaction between peptides that are oriented parallel to each other. However, interactions between helices oriented antiparallel with respect to each other are not detectable with this experiment. To investigate this possibility, we included two differently labeled WALP analogues in the assay, one labeled at the N terminus (pyr_N-WALP23), as described above, and one labeled at the C terminus (pyr_C-WALP23).

Fig. 2, *A* and *B*, shows the pyrene emission spectra for samples with a peptide/lipid ratio of 1/10. The pyrene emission for samples containing

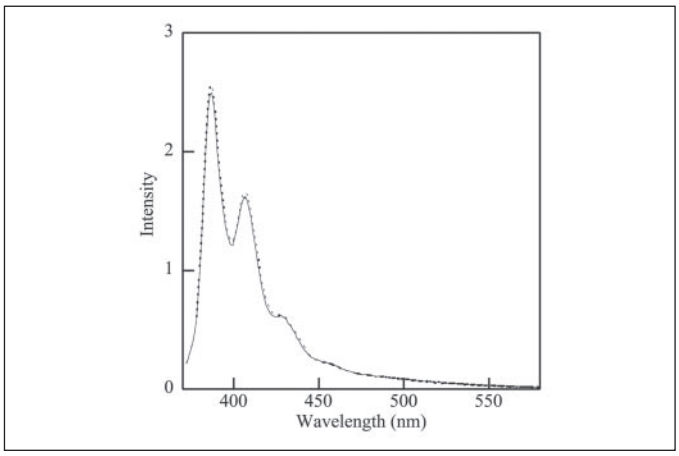

FIGURE 1. **Pyrene fluorescence spectra for the pyr_N-WALP23 in C18:1_c-PC bilayers.** Peptide/lipid ratios 1/10 (*solid line*) and 1/100 (*dotted line*).

only pyr_C-WALP23 was translated to slightly lower wavelengths than that of pyr_N-WALP23 (Fig. 2*A*), suggesting that the C terminus of the peptide exists in a slightly more hydrophobic environment (21) in the lipid bilayer. This is consistent with data from mass spectrometry (29), which showed that the C terminus is more protected from exchange than the N terminus, and from ESR measurements, suggesting that the peptide is slightly shifted with respect to the middle of the membrane (30). Importantly, excimer formation was not observed when only one type of these peptides was present, but when pyr_N-WALP23 and pyr_C-WALP23 were both present, excimer formation was observed (Fig. 2*B*). Maximum excimer intensity was obtained for the equimolar mixture of pyr_N-WALP23 and pyr_C-WALP23 (Fig. 2*C*). In principle, it is possible that these results are simply because of more favorable excimer formation by pyrene moieties in antiparallel peptides than in parallel peptides. However, this is unlikely, because we have previously shown that excimer formation also occurs in parallel peptides under certain conditions (18). Therefore, the most straightforward interpretation of our data is that there is only direct contact between antiparallel helices.

Next, pyrene fluorescence measurements were performed for samples with varying peptide/lipid ratios, ranging from 1/3000 to 1/10. The relationship between the excimer/monomer ratio (E/M) and the peptide concentration is shown in Fig. 2*D*. Excimer formation was detected at high peptide concentrations (peptide/lipid ratios above 1/25), and only when both types of peptides were present.

The influence of hydrophobic mismatch on helix-helix interactions was investigated by comparing the pyrene fluorescence for peptides incorporated in vesicles consisting of C14:1_c-PC (positive hydrophobic mismatch) or C22:1_c-PC (negative hydrophobic mismatch) to those obtained for C18:1_c-PC (hydrophobic match). Fig. 3*A* shows the pyrene emission spectra obtained for a peptide/lipid ratio of 1/25. We observed an increase in excimer intensity when there was hydrophobic mismatch between the peptides and the lipid bilayer. Excimer formation was also detected at slightly lower peptide concentrations than in the matching situation, with an offset at a peptide/lipid ratio of ~1/30 (Fig. 3*B*). This demonstrates that peptide aggregation is slightly promoted by hydrophobic mismatch. No difference was detected between the situations of negative and positive mismatch. Excimer formation only occurred when both types of peptides were present, indicating a preferred antiparallel organization of the interacting peptides regardless of the extent of hydrophobic mismatch.

Finally, increased peptide association was observed when WALP peptides were incorporated in C18:1_c-PC bilayers that included 40%

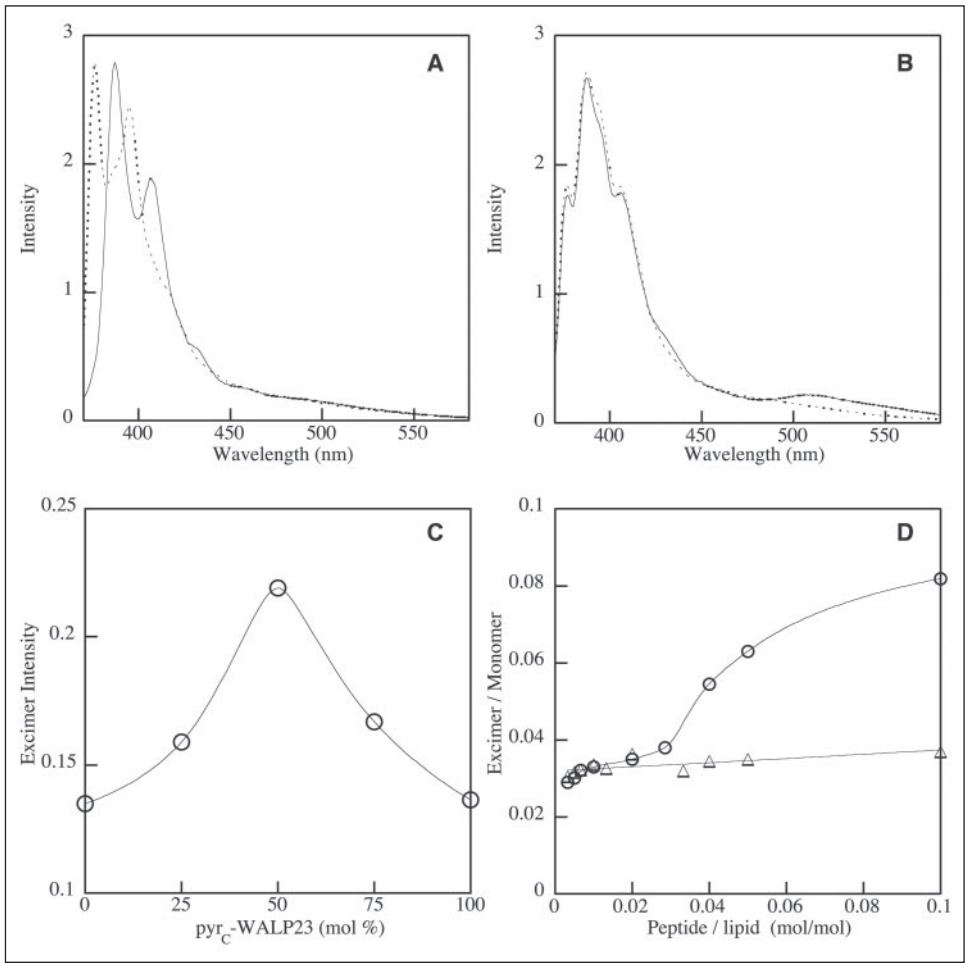

FIGURE 2. **Pyrene fluorescence data for pyrene-labeled WALP23 in C18:1$_c$-PC bilayers.** *A*, fluorescence spectra for the pyr$_N$-WALP23 (*solid line*) and pyr$_C$-WALP23 (*dotted line*) in DOPC vesicles, peptide/lipid ratio 1/10. *B*, fluorescence spectra of the equimolar mixture pyr$_N$-WALP23/pyr$_C$-WALP23 (*solid line*) in DOPC vesicles, peptide/lipid ratio 1/10, and the spectra calculated as the average of the spectra of pyr$_N$-WALP23 and pyr$_C$-WALP23 in *A* (*dashed line*). *C*, quantification of the excimer to monomer ratio (E/M) as a function of the pyr$_N$-WALP23/pyr$_C$-WALP23 ratio. *D*, excimer to monomer ratio (E/M) as a function of the peptide/lipid ratio for pyr$_N$-WALP23 (Δ) and for the equimolar mixture pyr$_N$-WALP23/pyr$_C$-WALP23 (○).

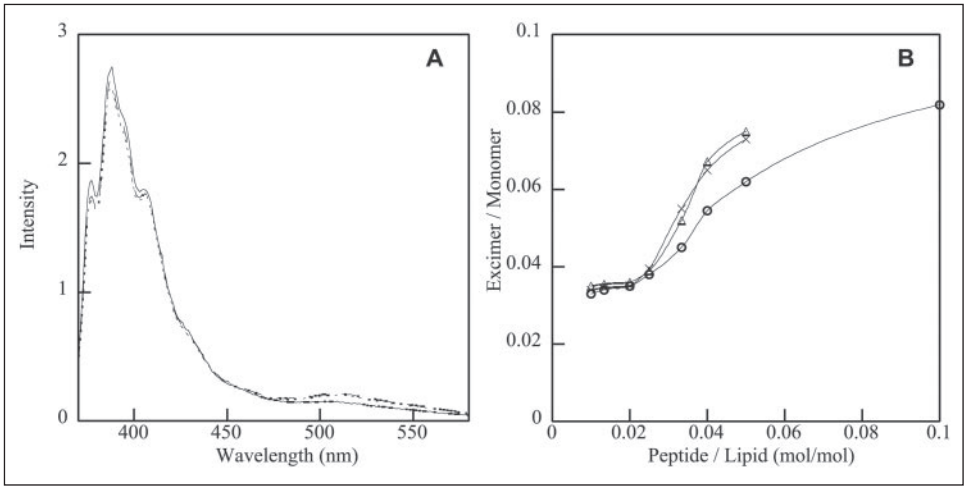

FIGURE 3. **Effect of hydrophobic mismatch on helix association.** *A*, pyrene fluorescence spectra for equimolar pyr$_N$-WALP23/pyr$_C$-WALP23 in vesicles of C18:1$_c$-PC (*solid line*), C14:1$_c$-PC (*dotted line*), and C22:1$_c$-PC (*dashed line*), peptide/lipid ratio 1/25. *B*, quantification of the excimer to monomer ratio (E/M) as a function of the peptide/lipid ratio for C18:1$_c$-PC (○), C14:1$_c$-PC (Δ), and C22:1$_c$-PC (×).

cholesterol (Fig. 4). This effect can be attributed to the increased hydrophobic mismatch because of thickening of the bilayer, as well as the increased lipid acyl chain order and the reduced area per phosphatidylcholine head group in the presence of cholesterol (31).

Helix-Helix Association as Analyzed by Fluorescence Resonance Energy Transfer—The interaction between helices was also investigated by FRET between Trp and pyrene, both of which are present in the labeled WALP peptides. The degree of Trp quenching increased at high peptide concentrations (Fig. 5*A*). These experiments were not expected to be sensitive to the antiparallel or parallel orientations of the interacting helices, as the peptides are flanked with Trp on both ends. Indeed, similar results were obtained when only one type of peptide, pyr$_N$-WALP23 or pyr$_C$-WALP23, was present, or when a mixture of peptides was present (data not shown). From this we can conclude that the labeling does not influence peptide-peptide interactions in a detectable way, and that helix association is not promoted by favorable pyrene interactions in one situation or the other.

The intermolecular FRET was also observed for bilayers of different thickness (Fig. 5*B*). Trp quenching was more efficient when the peptides

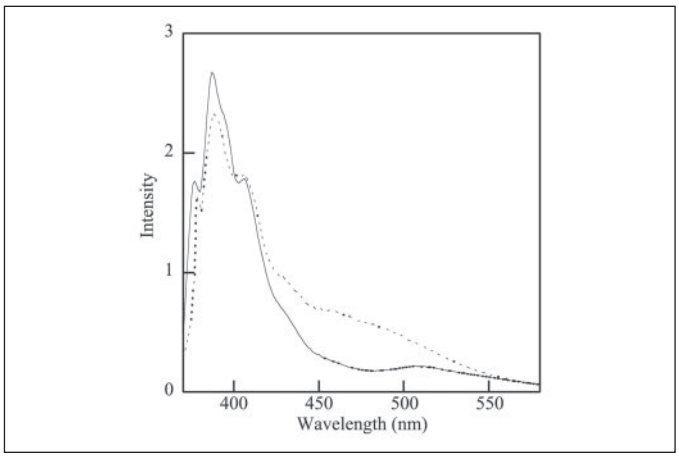

FIGURE 4. **The effect of cholesterol on helix association.** Pyrene fluorescence spectra for equimolar pyr_N-WALP23/pyr_C-WALP23 in vesicles of C18:1_c-PC (*solid line*), and C18:1_c-PC with 40% cholesterol (*dotted line*), peptide/lipid ratio 1/10.

were incorporated in bilayers of C14:1_c-PC and C22:1_c-PC, compared with when the peptides were present in vesicles composed of C18:1_c-PC. This is consistent with the results of our pyrene excimer fluorescence measurements.

Our observation that the Trp quenching increases with increasing peptide/lipid ratios implies a decreasing distance between the donors (Trp) and the acceptors (pyrene) (Fig. 5*B*). However, the experimental FRET data cannot be directly utilized to judge whether this effect is because of direct association between the peptides, or simply a consequence of the increased amount of randomly distributed peptides in the bilayer. To further investigate this, we performed a theoretical analysis of the same system, where the FRET was calculated for simulated systems with a random distribution of peptides and no intrinsic peptide-peptide association. The calculated FRET data (Fig. 5*B*, *dashed line*) show a good agreement in the case of the C18:1_c-PC vesicles, suggesting that the peptides are randomly distributed in the bilayer. However, unlike the real FRET measurements, the calculated FRET was found to be independent of the bilayer thickness (data not shown). Thus, the deviation between the experimental data and the calculated FRET in the situation of hydrophobic mismatch indicates that peptide aggregation is promoted when there is hydrophobic mismatch between the peptide and the lipids. This increase in peptide aggregation is only observed at peptide/lipid ratios above 1/30. At lower peptide concentrations the resemblance between the calculated and experimental FRET indicates random distribution of peptides in the bilayer, even in the case of hydrophobic mismatch. Furthermore, both the experimental and the calculated data show that the FRET is the same whether the peptide is labeled at the N or the C terminus.

Computer Modeling and Structure Prediction—We investigated the physical principles underlying WALP23 dimer formation and the molecular nature of these dimers with four computational models of both antiparallel and parallel dimers with both natural and modified backbone dipole arrangements. Interhelical separation distances and crossing angles in the models depended on the arrangement of the helix dipoles but not on whether the helices were physically parallel or antiparallel (Fig. 6*A*). Parallel dipoles resulted in greater interhelical separation (~1.1 nm) and larger crossing angles (±30°), antiparallel dipoles promoted closer packing (~0.8 nm) and a narrower distribution of crossing angles (with a peak near 0°). The identity of residues involved in inter-helical contacts also showed a dependence on the helix dipole orientation (TABLE ONE). Parallel dipoles resulted in a greater percentage of Leu contacts (54%) than antiparallel dipoles (50%), and fewer overall contacts within the ensemble (21,852 *versus* 29,046), demonstrating less extensive contact between helices.

Both the complete two-tiered clustering procedures (supplementary materials) and the simpler r.m.s. deviation clustering of representative subsets (Fig. 6*B*) showed that antiparallel dipole arrangements (AA and PA) resulted in more highly populated clusters than parallel dipoles (PP and AP). With antiparallel dipoles three well defined packing motifs were predicted: (i) a short stretch of Leu zipper involving residues Leu^{12} and Leu^{16} of one chain and Leu^{8} and Leu^{12} of the other chain, surrounded by Ala contacts at either termini (Fig. 7*A*), (ii) a short Leu zipper involving residues Leu^{4} and Leu^{8} of one chain and Leu^{16} and Leu^{20} of the other (Fig. 7*B*), and (iii) association in which all Ala residues along one face of each helix are closely packed (Fig. 7, *C* and *D*), with the helices almost perfectly aligned or slightly tilted. All three of these motifs were identified when the helix backbone dipoles were antiparallel to one another (AA and PA), regardless of the physical packing arrangement of the helices. With parallel dipoles (PP and AP) clustering analysis did not give rise to any highly represented packing arrangements, and these models resulted in very loosely packed dimers without full contact along the length of the helices (Fig. 7, *E* and *F*). These results indicate that the experimentally observed antiparallel association of helices is a result of favorable electrostatic interactions between the α-helix backbone dipole moments in the antiparallel dimer.

DISCUSSION

Interaction between Antiparallel Peptides—The internal organization of interacting helices is fundamental to protein association and protein folding. This can be regulated by relatively strong and specific interactions including the formation of interhelical hydrogen bonds and favorable side chain packing, and electrostatic interactions between charged residues (5, 9, 32). In the situation investigated here, none of these forces are present, and we expect that the internal organization of the associated peptides is determined by relatively weak interactions between the helices and unfavorable packing interactions between the peptides and lipids. This might in fact be a representative situation for the arrangement of helices in polytopic membrane proteins, where in many cases specific recognition motifs cannot be identified. However, even in cases where TM helices do contain such recognition motifs, the nonspecific interactions discussed here will still contribute to the total energy of association between the helices.

The WALP peptides are readily incorporated in liquid crystalline lipid bilayers as membrane-spanning α-helices (16). From the pyrene fluorescence experiments we can conclude that association almost exclusively occurs between peptides that are oriented antiparallel with respect to each other. This is true for all different peptide concentrations and all lipid compositions investigated. Formation of antiparallel dimers has also been proposed for the unflanked TM Ac-$(LALAAAA)_3$-amide analogue, based on dithionite quenching experiments (33), suggesting that antiparallel association is a generic property for these types of interacting TM α-helices.

What would be the reason for this antiparallel packing? A possible explanation arises from the observation that the peptide α-helices have a macrodipole moment (34–36). The nature and importance of this dipole moment is still a matter of some controversy, with some studies suggesting that the observed dipole effect in some proteins is a local effect confined to the termini (37). One theoretical investigation of poly-Ala helix association using a simplified bilayer representation suggested that dipole-dipole interactions are quite weak, because of solvent and counterion screening of the partially charged helix termini (38). Our proposal is that although these interactions might be relatively weak,

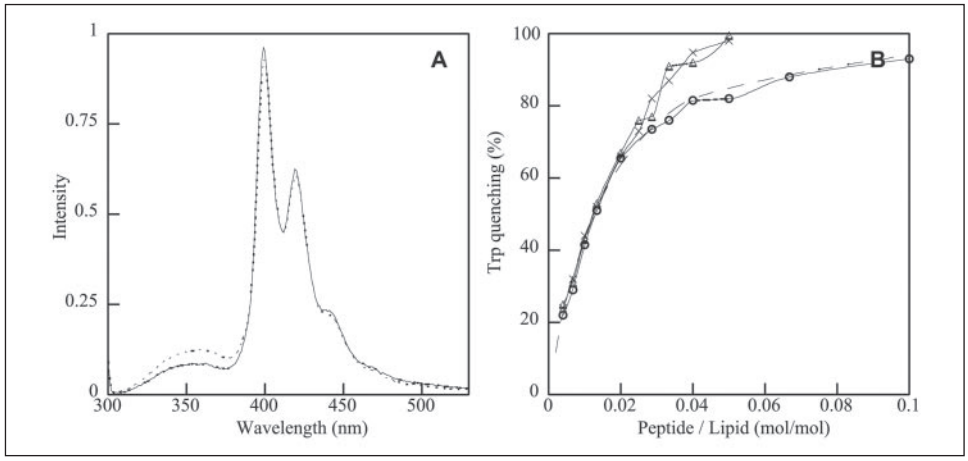

FIGURE 5. **FRET from Trp to pyrene.** *A*, FRET measured for pyr_N-WALP23 in C18:1_c-PC bilayers, peptide/lipid ratios 1/10 (*solid line*) and 1/100 (*dotted line*). *B*, quantification of the FRET data measured for pyr_N-WALP23 in vesicles of C18:1_c-PC (○), C14:1_c-PC (×), and C22:1_c-PC (Δ); intermolecular Trp quenching (%) as a function of peptide/lipid ratio. The experimental data are compared with calculated FRET data for pyr_N-WALP23 in a bilayer with thickness 3.0 nm, corresponding to C18:1_c-PC (*dashed line*).

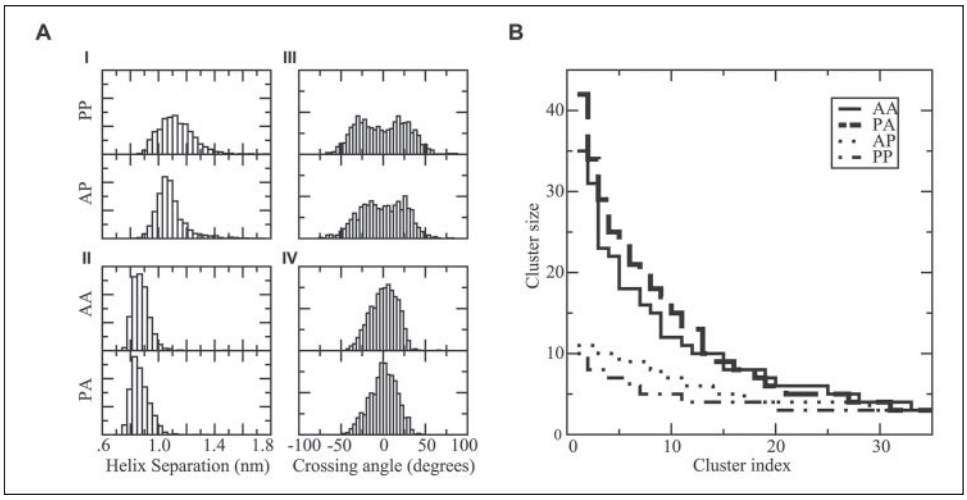

FIGURE 6. **Summary of computer models.** *A*, dimer interhelical separation (*I* and *II*) and crossing angle (*III* and *IV*) distributions. *PP*, parallel packing, parallel dipole; *AP*, antiparallel packing, parallel dipole; *AA*, antiparallel packing, antiparallel dipole; *PA*, parallel packing, antiparallel dipole. *B*, cluster size distribution for a representative subset of the modeling data (500 structures from each model, all non-hydrogen atoms, r.m.s. deviation cut-off 0.3 nm). *Solid line*, AA; *dashed line*, AP; *dot-dot line*, PP; *dot-dash line*, PA. The top structures fall into the same structural classes as those shown in Fig. 7.

TABLE ONE

Total number of interhelical contacts (d < 0.4 nm) by residue type

	Antiparallel dipoles				Parallel dipoles			
	AA	PA	Average	Fraction	PP	AP	Average	Fraction
Ala	14,633	14,455	14,544	0.5007	10,157	9,844	10,000	0.4576
Leu	14,512	14,492	14,502	0.4993	11,918	11,787	11,852	0.5424

they are strong enough to specify antiparallel association in the absence of stronger, specific helix association forces. The importance of solvent screening of the helix termini may also be lower in cases where helices are constrained to be in close contact by high local peptide concentration or the topology of a polytopic membrane protein. This has important implications for understanding the folding and association of proteins in biological membranes. Antiparallel orientations of adjacent helices are preferred over parallel orientations in known structures of membrane proteins (39, 40).

Our computer models showed that antiparallel peptides form well packed dimers, whereas parallel peptides are loosely packed and have a lower tendency to form ordered structures. These tendencies are clearly dependent on the backbone dipole orientations, but not on the physical packing orientation of the helices, which allows us to rule out the possibility of a preferred steric packing arrangement between WALP helices. This is also suggested by the sequence symmetry of the WALP peptide. Modeling indicates three possible ordered packing motifs. Although it is not possible to determine the distribution between these modes in a membrane using this model, clustering analysis suggests that the central Leu zipper (Fig. 7*A*) involving Leu^{16}/Leu^{12} and Leu^{8}/Leu^{12} is the most favorable. This modeling procedure was done in vacuum. However, the applicability of this approach to simple transmembrane proteins such as glycophorin A (41), and the consistency of the results with the experimental observations outlined above, suggest that the approximations used are applicable to this specific system.

The interacting peptides in this system form antiparallel dimers rather than larger oligomers. Larger aggregates would involve both parallel and antiparallel interactions between helices, which are not observed in our experiments. Dimer formation, rather than trimer or oligomer formation, has also been proposed for Trp- or dibromotyrosine-containing Lys-flanked poly-Leu peptide analogues in liquid crystalline bilayers (12). This is also in agreement with previous ESR measurements, which indicated that WALP and L_{24} (Ac-$K_2L_{24}K_2$-amide) peptides are present as monomers or dimers, even at high peptide/lipid ratios (20, 42, 43).

Our results have implications for the folding and assembly of membrane proteins. Folding of polytopic membrane proteins involves interactions between both parallel and antiparallel helix pairs, and it can

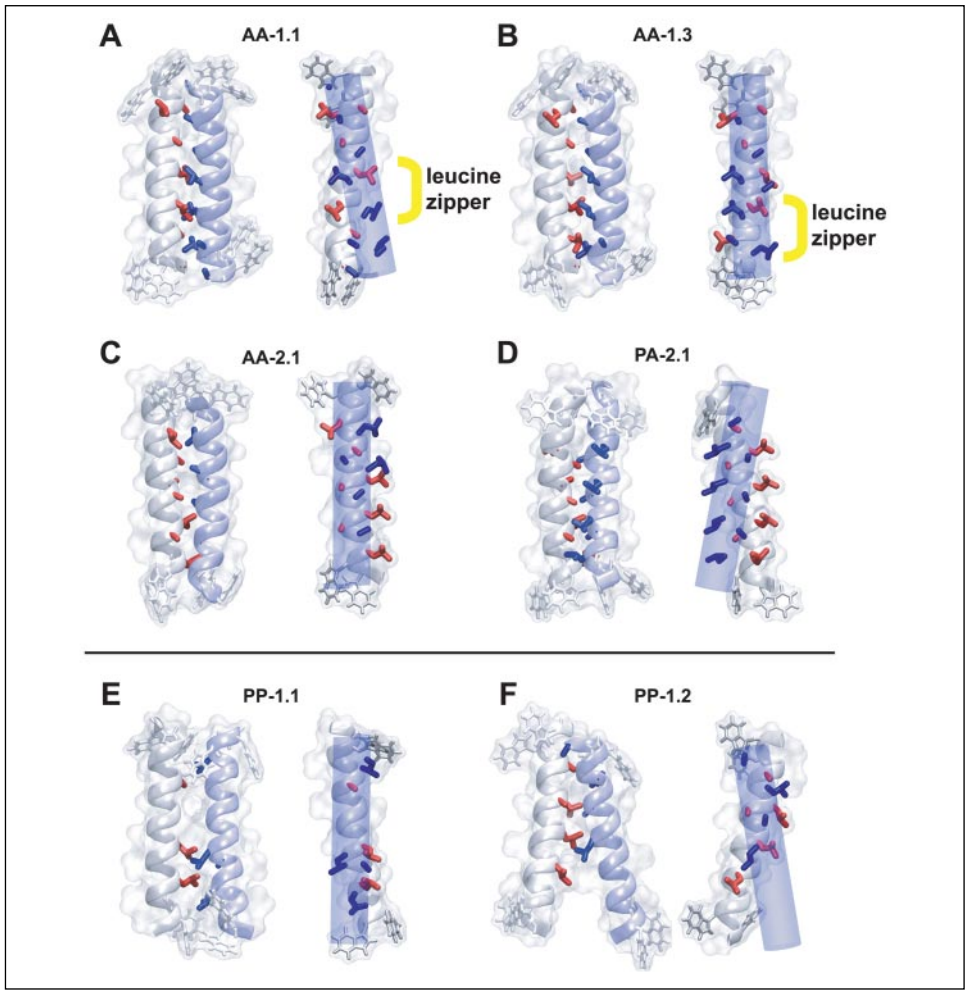

FIGURE 7. **Predicted structures for antiparallel helix dimers (*top*), and illustration of poor packing seen for parallel helix dimers (*bottom*).** Each model is shown in two views related by a 90 degree rotation. Residues that form intermonomer contacts (at least two atom-atom distances less than 0.4 nm) are highlighted in *red* and *blue*. *A* and *B*, two structures with a short two-turn Leu zipper flanked by Ala contacts along the remainder of the helices. *C* and *D*, structures with mainly Ala contact, with helices aligned or tilted. Leu residues slightly outside of the interface can still form contacts in these arrangements. *E* and *F*, poor packing typically observed in the parallel dipole models. The model as well as cluster and subcluster identity (*e.g.* cluster 1 and subcluster 1 = 1.1) is identified *above* each structure.

therefore be expected that the favorable antiparallel packing of helices significantly contributes to the overall structure of proteins and to their stability. Although these interactions appear to be relatively weak, they are strong enough to specify antiparallel association over parallel association when hydrophobic mismatch or high peptide concentration induces contact between peptides. This may be analogous to the locally high concentration of helices imposed by the connecting loops in a polytopic membrane protein, and thus may influence the overall architecture of proteins.

In contrast, self-association of monotopic membrane proteins typically involves interactions between helices that are aligned in a parallel fashion. For such assemblies specific recognition motifs are expected to occur, and indeed have been reported (5, 6, 41). This may be essential to overcome the otherwise less favorable packing of parallel helices.

Hydrophobic Mismatch Promotes Helix-Helix Association—From the combined experimental and theoretical analysis of the FRET data on helix-helix interactions in the matching C18:1_c-PC bilayers, we conclude that the WALP peptides have no intrinsic tendency to aggregate in liquid crystalline lipid bilayers, except at high peptide concentration. Thus, the interaction between helix dipole moments is not sufficient to induce aggregation of the helices in the bilayer. However, in cases where there is negative or positive hydrophobic mismatch between the peptides and the bilayer, either because of increased chain length of the lipids or the inclusion of cholesterol, peptide association is promoted. In these situations peptide-peptide interactions become more favorable than peptide-lipid interactions.

Peptide aggregation induced by hydrophobic mismatch has previously been observed for Lys-flanked analogues by fluorescence measurements (15, 44). Thus, it seems to be a general property of mismatching peptides. However, the Lys-flanked peptides appear to have a stronger tendency to associate at negative mismatch and they form larger oligomeric aggregates than the WALP peptides (17). A possible explanation for this would be that Lys residues are more flexible and may better accommodate oligomerization of the peptides than the more bulky Trp residues. In any case, the molecular details of interacting helices are clearly important in modulating the effects of changing the lipid environment, sometimes in very subtle ways.

Peptide oligomerization induced by hydrophobic mismatch and the presence of cholesterol is likely to play a role in the biology of membrane proteins, for example, in signaling processes where clustering of receptor proteins is related to partitioning into raft-like domains (45, 46). Because of the high cholesterol content and the long chains of the sphingolipids in these raft-like domains, they are expected to be thicker than the surrounding membrane, in which the proteins would be mainly present as monomers. Here, less favorable interactions between the lipids and the receptor proteins may help to accommodate the oligomerized form into these raft-like domains.

Conclusion—Helix-helix association is a key event in many cellular processes involving folding and assembly of membrane proteins. The extent of helix-helix association and the nature of this association clearly depends on multiple factors, all of which contribute to the total energy of helix association and thus to the folding and function of mem-

brane proteins and protein complexes. Our study shows that two such factors are the favorable interactions between antiparallel helices, and the balance between lipid-protein and protein-protein interactions.

REFERENCES

1. Arkin, I. T. (2002) *Biochim. Biophys. Acta* **1565,** 347–363
2. Chamberlain, A., Faham, S., Yohannan, S., and Bowie, J. (2003) in *Advances in Protein Chemistry* (Rees, D. C., ed) Vol. 63, pp. 19–46, Academic Press, Amsterdam
3. Engelman, D. M., Chen, Y., Chin, C. N., Curran, A. R., Dixon, A. M., Dupuy, A. D., Lee, A. S., Lehnert, U., Matthews, E. E., Reshetnyak, Y. K., Senes, A., and Popot, J. L. (2003) *FEBS Lett.* **555,** 122–125
4. Langosch, D., Lindner, E., and Gurezka, R. (2002) *IUBMB Life* **54,** 109–113
5. Zhou, F. X., Merianos, H. J., Brunger, A. T., and Engelman, D. M. (2001) *Proc. Natl. Acad. Sci. U. S. A.* **98,** 2250–2255
6. Choma, C., Gratkowski, H., Lear, J. D., and DeGrado, W. F. (2000) *Nat. Struct. Biol.* **7,** 161–166
7. Johnson, R. M., Heslop, C. L., and Deber, C. M. (2004) *Biochemistry* **43,** 14361–14369
8. MacKenzie, K. R., Prestegard, J. H., and Engelman, D. M. (1997) *Science* **276,** 131–133
9. Senes, A., Ubarretxena-Belandia, I., and Engelman, D. M. (2001) *Proc. Natl. Acad. Sci. U. S. A.* **98,** 9056–9061
10. Lee, A. G. (2004) *Biochim. Biophys. Acta* **1666,** 62–87
11. Killian, J. A. (1998) *Biochim. Biophys. Acta* **1376,** 401–416
12. Mall, S., Broadbridge, R., Sharma, R. P., East, J. M., and Lee, A. G. (2001) *Biochemistry* **40,** 12379–12386
13. Orzáez, M., Lukovic, D., Abad, C., Pérez-Payá, E., and Mingarro, I. (2005) *FEBS Lett.* **579,** 1633–1638
14. Webb, R. J., East, J. M., Sharma, R. P., and Lee, A. G. (1998) *Biochemistry* **37,** 673–679
15. Ren, J. H., Lew, S., Wang, J. Y., and London, E. (1999) *Biochemistry* **38,** 5905–5912
16. Killian, J. A. (2003) *FEBS Lett.* **555,** 134–138
17. de Planque, M. R. R., and Killian, J. A. (2003) *Mol. Membr. Biol.* **20,** 271–284
18. Sparr, E., Ganchev, D. N., Snel, M. M. E., Ridder, A. N. J. A., Kroon-Batenburg, L. M. J., Chupin, V., Rijkers, D. T. S., Killian, J. A., and de Kruijff, B. (2005) *Biochemistry* **44,** 2–10
19. Rouser, G., Fleisher, S., and Yamamoto, A. (1970) *Lipids* **5,** 494–496
20. de Planque, M. R. R., Kruijtzer, J. A. W., Liskamp, R. M. J., Marsh, D., Greathouse, D. V., Koeppe, R. E., de Kruijff, B., and Killian, J. A. (1999) *J. Biol. Chem.* **274,** 20839–20846
21. Lakowicz, J. R. (1999) *Principles in Fluorescence Spectroscopy*, Kluwer Academic/Plenum Publishers, New York
22. Yatskou, M. M., Donker, H., Koehorst, R. B. M., van Hoek, A., and Schaafsma, T. J. (2001) *Chem. Phys. Lett.* **345,** 141–150
23. Nazarov, P. V., Apanasovich, V. V., Lutkovski, V. M., Yatskou, M. M., Koehorst, R. B. M., and Hemminga, M. A. (2004) *J. Chem. Inf. Comput. Sci.* **44,** 568–574
24. Nilges, M., and Brunger, A. T. (1993) *Proteins* **15,** 133–146
25. Ash, W. L., Stockner, T., MacCallum, J. L., and Tieleman, D. P. (2004) *Biochemistry* **43,** 9050–9060
26. Strelkov, S. V., and Burkhard, P. (2002) *J. Struct. Biol.* **137,** 54–64
27. Seo, J., and Shneiderman, B. (2004) *Proc. IEEE Inf. Vis.* **2004,** 65–72
28. Kelley, L. A., Gardner, S. P., and Sutcliffe, M. J. (1996) *Protein Eng.* **9,** 1063–1065
29. Demmers, J. A. A., Haverkamp, J., Heck, A. J. R., Koeppe, R. E., and Killian, J. A. (2000) *Proc. Natl. Acad. Sci. U. S. A.* **97,** 3189–3194
30. Nielsen, R. D., Che, K., Gelb, M. H., and Robinson, B. H. (2005) *J. Am. Chem. Soc.* **127,** 6430–6442
31. Vist, M. R., and Davis, J. H. (1990) *Biochemistry* **29,** 451–464
32. Lew, S., Caputo, G. A., and London, E. (2003) *Biochemistry* **42,** 10833–10842
33. Yano, Y., Takemoto, T., Kobayashi, S., Yasui, H., Sakurai, H., Ohashi, W., Niwa, M., Futaki, S., Sugiura, Y., and Matsuzaki, K. (2002) *Biochemistry* **41,** 3073–3080
34. Hol, W. G. J., Vanduijnen, P. T., and Berendsen, H. J. C. (1978) *Nature* **273,** 443–446
35. Hol, W. G. J. (1985) *Adv. Biophys.* **19,** 133–165
36. Sansom, M. S. P. (1991) *Prog. Biophys. Mol. Biol.* **55,** 139–235
37. Aqvist, J., Luecke, H., Quiocho, F. A., and Warshel, A. (1991) *Proc. Natl. Acad. Sci. U. S. A.* **88,** 2026–2030
38. Ben-Tal, N., and Honig, B. (1996) *Biophys. J.* **71,** 3046–3050
39. Gimpelev, M., Forrest, L. R., Murray, D., and Honig, B. (2004) *Biophys. J.* **87,** 4075–4086
40. Bowie, J. U. (1997) *J. Mol. Biol.* **272,** 780–789
41. Treutlein, H. R., Lemmon, M. A., Engelman, D. M., and Brunger, A. T. (1992) *Biochemistry* **31,** 12726–12733
42. de Planque, M. R. R., Greathouse, D. V., Koeppe, R. E., Schafer, H., Marsh, D., and Killian, J. A. (1998) *Biochemistry* **37,** 9333–9345
43. Subczynski, W. K., Lewis, R., McElhaney, R. N., Hodges, R. S., Hyde, J. S., and Kusumi, A. (1998) *Biochemistry* **37,** 3156–3164
44. Mall, S., Broadbridge, R., Sharma, R. P., Lee, A. G., and East, J. M. (2000) *Biochemistry* **39,** 2071–2078
45. Rajendran, L., and Simons, K. (2005) *J. Cell Sci.* **118,** 1099–1102
46. Pike, L. J. (2003) *J. Lipid Res.* **44,** 655–667